

Article

# Topological Indices, Graph Spectra, Entropies, Laplacians, and Matching Polynomials of n-Dimensional Hypercubes

Krishnan Balasubramanian

School of Molecular Sciences, Arizona State University, Tempe, AZ 85287-1604, USA; baluk@asu.edu

**Abstract:** We obtain a large number of degree and distance-based topological indices, graph and Laplacian spectra and the corresponding polynomials, entropies and matching polynomials of n-dimensional hypercubes through the use of Hadamard symmetry and recursive dynamic computational techniques. Moreover, computations are used to provide independent numerical values for the topological indices of the 11- and 12-cubes. We invoke symmetry-based recursive Hadamard transforms to obtain the graph and Laplacian spectra of nD-hypercubes and the computed numerical results are constructed for up to 23-dimensional hypercubes. The symmetries of these hypercubes constitute the hyperoctahedral wreath product groups which also pave the way for the symmetry-based elegant computations. These results are used to independently validate the exact analytical expressions that we have obtained for the topological indices as well as graph, Laplacian spectra and their polynomials. We invoke a robust dynamic programming technique to handle the computationally intensive generation of matching polynomials of hypercubes and compute all matching polynomials up to the 6-cube. The distance degree sequence vectors have been obtained numerically for up to 108-dimensional cubes and their frequencies are found to be in binomial distributions akin to the spectra of n-cubes.

**Keywords:** hypercubes; topological indices; graph spectra of hypercubes; matching polynomials of hypercubes; Laplacian spectra of hypercubes; spanning trees of hypercubes; hadamard transform; symmetries of hypercubes

**Citation:** Balasubramanian, K.Topological Indices, Graph Spectra, Entropies, Laplacians, and Matching Polynomials of n-Dimensional Hypercubes. *Symmetry* **2023**, *15*, 557. <https://doi.org/10.3390/sym15020557>

Academic Editor: Markus Meringer

Received: 30 January 2023

Revised: 12 February 2023

Accepted: 17 February 2023

Published: 20 February 2023



**Copyright:** © 2023 by the author. Licensee MDPI, Basel, Switzerland. This article is an open access article distributed under the terms and conditions of the Creative Commons Attribution (CC BY) license (<https://creativecommons.org/licenses/by/4.0/>).

## 1. Introduction

Hypercubes are highly symmetric structures that have been the focus of numerous studies due to their varied applications in many fields such as artificial intelligence, parallel architectures, recursive structures, the last Fermat's theorem, Minkowski norm, neural networks, big data, genetic regulatory networks, the periodic table of elements, phylogenetic trees, moonlighting functions of intrinsically disordered proteins, water clusters, and so forth [1–40]. In the context of molecular science and drug discovery, hypercubes have been employed to partition big data sets [9,12,27–30] into equivalence classes [12,27–30,38–40], biochemical imaging [13–15], and in the representations of symmetries of nonrigid molecules and water clusters [23–32]. Water clusters exhibit semi-rigid to nonrigid structures owing to their potential energy surfaces that contain multiple minima divided by surmountable potential energy barriers. Consequently, the assignments of the observed spectra, nuclear spin species, and tunneling splittings in the spectra require symmetries of nonrigid groups molecules that are represented by the automorphism groups of hypercubes or wreath product groups in the nonrigid limit [23–32,34–36]. Moreover, the observed transient chirality in water clusters is akin to the spontaneous generation of optical activity of molecules exhibiting rapid internal rotations whose rotation digraphs are finite topologies and Borel fields [27]. The symmetries of non-rigid molecules and the NMR groups of NMR graphs are all connected to symmetries of nonrigid molecules and those of hypercubes [23–32,34–37]. The subject matters of hypercubes, polycubes and wreath product groups have been dealt with by several researchers over the years [1–40], including techniques to obtain topological

indices [41–50] by cut methods which involve subgraphs of hypercubes [41,42]. Furthermore, graph spectra, matching polynomials, distance degree sequences, topological indices and other properties of graphs pertinent to chemical applications have been the subject matter of several studies [51–67].

The recursive hypercube-like structures appear in phylogenetic trees [68] as well as pandemic trees that have been applied to the analysis of propagation and the dynamics of the SARS-CoV-2 epidemic [20]. Forster et al. [21] have shown that phylogenetic network analysis of SARS-CoV-2 genomes can enhance our understanding of the genetic evolution of the SARS-CoV-2 virus, its variation as a function of geographical regions and its graph-theoretical connection to the presumed bat origin. Such graph-theoretical networks, cluster graphs, and Cayley trees have been employed in statistical analysis of networks, fuzzy logic, contact tracing and Boolean networks [20,21]. The recursive trees of biological interest that appear in the context of genetic regulatory networks and intrinsically disordered proteins exhibit hypercube symmetries which are wreath products [12,16–22].

The computations of topological indices [41–50], graph spectra [51,52] and perfect matchings [53,54] of clusters, graphs and hypercubes can be challenging, and thus the topic has received some attention over the years. A few topological indices such as the Wiener, Szeged, Balaban, and Kirchhoff indices of the hypercubes have been obtained before [46–51]. Likewise, the constant coefficients of the matching polynomials which generate the numbers of perfect matchings have been considered for a few hypercubes up to 7-cube [53,54]. The computation of the matching polynomials is one of the most intensive problems, as described previously. The hypercube graphs are extremely clustered, and thus offer significant challenges for the computations of matching polynomials of nD-hypercubes.

The focus of the present study is to explore the topological indices of nD-hypercubes in an exhaustive manner in that we consider both distance and degree-based indices including some recently introduced indices based on both distance degrees and vertex degrees such as the Sombor index, RMS-Sombor index, geometric-mean Szeged index as well as edge, vertex, vertex-edge and total versions of these indices. We have computed the topological indices and compiled numerical tables of these indices for up to 12-cubes. Moreover, we have obtained the exact analytic expressions of these indices for any nD-hypercube. Likewise, the graph spectra, Laplacian spectra, spectral polynomials and Laplacian polynomials of hypercubes up to dimension 23 have been numerically computed without the use of any factorings of characteristic polynomials. A number of properties including graph energies and the number of spanning trees of nD-hypercubes have been numerically enumerated. We have employed an elegant recursive Hadamard transform to compute the spectra of nD-hypercubes which form elegant binomially symmetric patterns for both Laplacian and graph spectra. Powerful dynamical computer algorithms are employed to compute the matching polynomials of nD-hypercubes, and explicit tables of the matching polynomials have been constructed for up to 6-dimensional hypercubes and prime factors of the constant coefficients are explicitly constructed.

## 2. Mathematical and Computational Techniques for Topological and Spectral Properties of Hypercubes

Hypercubes are recursive structures in an n-dimensional space with  $2^n$  vertices. As an illustration, we show three panels in Figure 1 where the first panel is a representation of a 4-dimensional hypercube with 16 vertices. Figure 1b shows one of the potential minima of water octamer, while Figure 1c shows an 8-cube octeract representation with 256 vertices that also correspond to 256 potential energy minima of water octamer. At higher temperatures the hydrogen bonds in Figure 1b are broken and remade, thus lending a nonrigid character for the water octamer. Likewise, Figure 1a vertices represent the sixteen potential minima of water tetramer, and thus the automorphism group of the graph in Figure 1a, the wreath product  $S_4[S_2]$ , yields the symmetry group of nonrigid water

tetramer. Thus, hypercubes play an important role in the representations of symmetry groups of such nonrigid molecules.

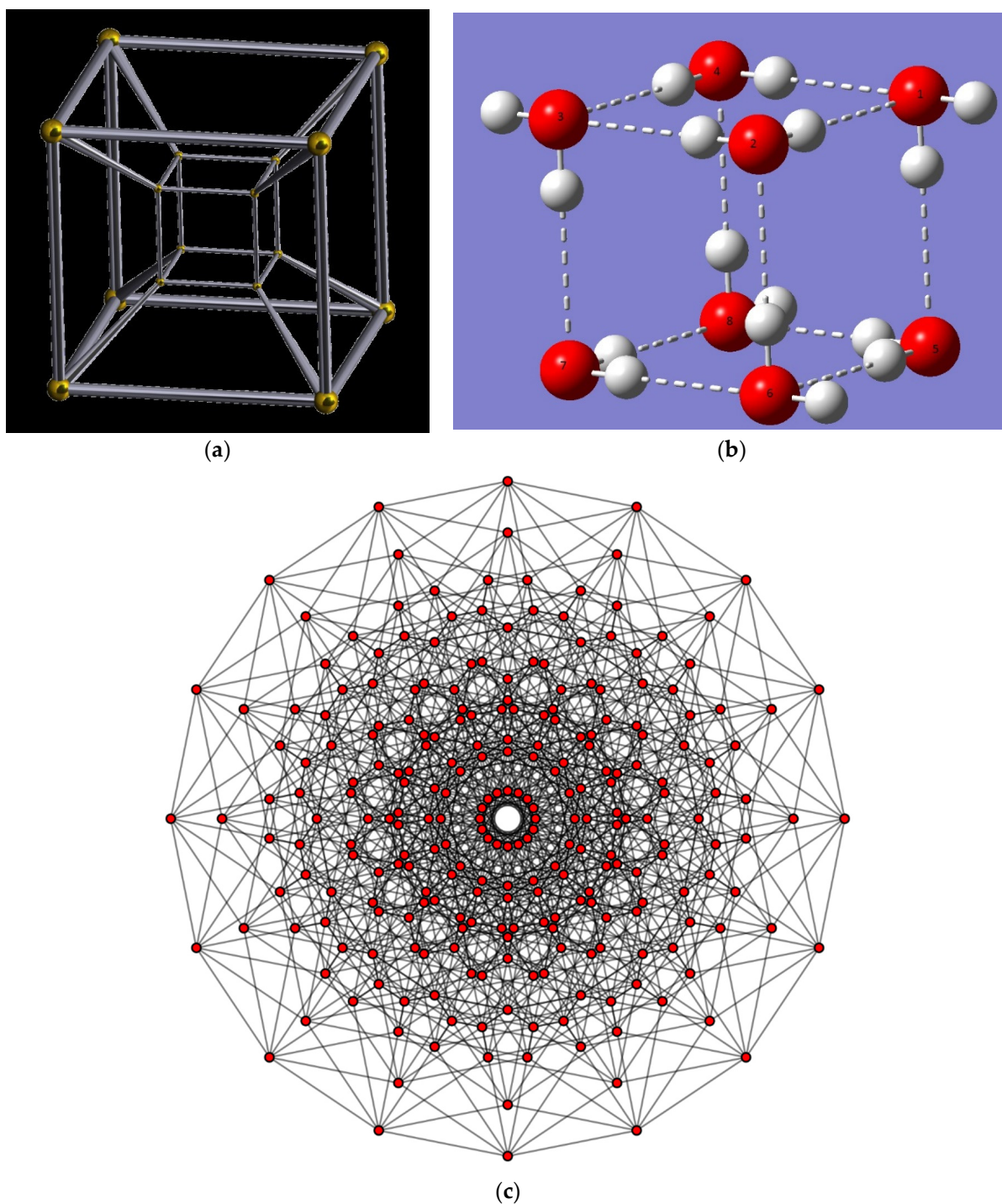


**Figure 1.** (a) A representation of the 4D-hypercube; (b) The  $S_4$  isomer of  $(\text{H}_2\text{O})_8$  and in relationship to an ideal cubic arrangement; Reproduced from [69] (c) the graph of the 8-cube octeract representation of water octamer with 256 vertices and 1024 edges. (c) reproduced from Tom Ruen, open source, copyright free, Public Domain Image: <https://commons.wikimedia.org/wiki/File:8-cube.svg>, accessed on 28 January 2023.

Following Harary [55], an  $n$ -dimensional hypercube denoted by  $Q_n$ , is recursively constructed by the Cartesian product:

$$Q_n = Q_{n-1} \times K_2 \text{ for } n \geq 2 \text{ with } Q_1 = K_2,$$

where  $K_2$  is simply a graph of two vertices connected by an edge. This recursive construction can be computationally transcribed into a recursive construction of the adjacency matrices of hypercubes by invoking the adjacency matrices of hypercubes of lower order. That is, the adjacency matrix of  $Q_{n+1}$ ,  $A_{Q_{n+1}}$ , is given by:

$$A_{Q_{n+1}} = \begin{bmatrix} A_{Q_n} & I \\ I & A_{Q_n} \end{bmatrix}$$

where  $I$  is simply the identity matrix of order  $2^n \times 2^n$ .

The above recursive construction makes it very tractable to construct adjacency matrices of  $nD$ -hypercubes quite rapidly. Note that the number of  $q$ -hyperplanes of an  $n$ -cube with  $0 \leq q \leq n - 1$  is given by  $C_{qq}$ , the diagonal elements of the Coxeter configuration matrix of the  $n$ -cube, and it is given by:

$$C_{qq} = \binom{n}{q} 2^{n-q}$$

Thus, the no. of vertices ( $q = 0$ ) of an  $n$ -cube is  $2^n$  while the number of edges of an  $n$ -cube ( $q = 1$ ) is  $n \times 2^{n-1}$ . For example, a 12-cube contains  $2^{12} = 4096$  vertices and 24,576 edges and so on. Thus, by the time we reach  $n = 23$ , the largest dimension considered in the present study for computations, the numbers of vertices and edges become 8,388,068 and 94,468,992, indicating the combinatorial and computational complexity of the  $n$ -cube problem.

In order to derive the topological indices that are distance based we need to compute the distance matrices from the adjacency matrices. For the present problem of  $nD$ -hypercubes, we employ the author’s previously developed computational techniques [56,57] based on Frame’s method for the spectral polynomials. The algorithm is polynomial in order and converges rapidly within  $r - 1$  iterations where  $r$  is the radius of the  $n$ -cube which is simply  $n$ . Consequently, the distance matrix of a 12-cube, for example, is constructed in 11 iterations in our computational algorithm. Once the distance matrix is constructed together with the adjacency matrix, several of the topological indices such as the Wiener index, hyper-Wiener index, Balaban’s index, ABC index, Randić index, Harary index, etc., are computed. However, the computations of other indices such as the Szeged index, Padmakar–Ivan index and their edge as well as vertex-edge variants require computations of additional neighborhood parameters denoted by  $n_u, n_v, m_u$  and  $m_v$  as defined in Refs. [41,42]. All of these indices are obtained by summing over the edges of the hypercube, and thus require  $n \times 2^{n-1}$  multiplications in the summations. Thus, the computation of these distance-based edge indices is a computationally more intensive problem, requiring multiple nested loops over the vertices, although only if there is an edge between vertices  $u$  and  $v$  do the arithmetic operations need to be carried out.

Table 1 shows a list of topological indices considered here with their expressions for computing them. As can be seen from Table 1, we have considered a large number of topological indices, some of which are vertex-degree based while the others are based on topological distances. There are a few more indices that we have computed but their definitions are available in references [41,42]. We note that we have introduced variants of the recently introduced Sombor indices using the distance degrees or distance status [43] as derived from the distance matrices of  $n$ -cubes (see Table 1, Sombor (DD)). The scaled and root-mean-square versions of these indices are also considered. The entropies can be defined for each topological index based on information-theoretic expressions of Shannon [41,42]. However, for  $n$ -cubes all the entropies for various topological indices reduce to a single expression.

**Table 1.** The topological indices Considered for the n-cubes with u and v defined as vertices and E(G) as the set of edges and V(G) as the set of vertices of the hypercube graph  $G = Q_n^a$ .

Index	Expression
Wiener Index	$W(G) = \sum_{\{u,v\} \subset V(G)} d(u,v).$
Schultz Index	$d_u = \sum_{v \subset V(G)} a_{uv}$ $SI(G) = \frac{1}{2} \sum_{\{u,v\} \subset V(G)} (d_u + d_v).d(u, v)$
Hyper-Wiener Index	$WW(G) = \frac{1}{2}W(G) + \frac{1}{2} \sum_{\{u,v\} \subset V(G)} d(u, v)^2$
M1(Zagreb)	$M_1 = \sum_{uv \in E(G)} (d_u + d_v), \quad d_u = \sum_{v \subset V(G)} a_{uv}$
M2(Zagreb)	$M_2 = \sum_{uv \in E(G)} (d_u d_v)$
Harary Index	$H(G) = \sum_{u,v \in V(G)} \frac{1}{d(u,v)}$
RMS Distance Index	$RMS(D) = \sqrt{\frac{1}{ V(G) } \sum_{\{u,v\} \subset V(G)} d(u, v)^2}$
Randić Index	$R = \sum_{uv \in E(G)} \sqrt{\frac{1}{d_u d_v}}, \quad d_u = \sum_{v \subset V(G)} a_{uv}$
Cubic Vertex Degree Sum	$CVD = \sum_{u \in V(G)} d_u^3,$
ABC Index	$ABC = \sum_{uv \in E(G)} \sqrt{\frac{d_u + d_v - 2}{d_u * d_v}}$ $d_u = \sum_{v \subset V(G)} a_{uv}$
Balaban Index	$J = \frac{m}{\gamma + 1} \sum_{(uv) \in E(G)} (\delta_u \delta_v)^{-\frac{1}{2}}, \gamma = m - n + c, \delta_u = \sum_{v \ni (uv) \in E(G)} d(u, v),$ $n =  V(G) , m =  E(G) , c = \text{number of connected components}$
Szeged Index(v)	$n_u = n_u(e G) = \{x \in V(G) : d(u, x) < d(v, x)\}$ $n_v = n_v(e G) = \{x \in V(G) : d(v, x) < d(u, x)\}$ $Sz_v(G) = \sum_{uv \in E(G)} n_u(e G) n_v(e G),$
Padmakar–Ivan (v)	$PI_v(G) = \sum_{uv \in E(G)} (n_u(e G) + n_v(e G)),$
Geometric-Mean-Szeged(v)	$SZ_v^{GM}(G) = \sum_{uv \in E(G)} \sqrt{n_u(e G)n_v(e G)}$
Szeged Index(e)	$e = uv \in E(G), m_u = m_u(e G) = \{x \in E(G) : d(u, x) < d(v, x)\},$ $m_v = m_v(e G) = \{x \in E(G) : d(v, x) < d(u, x)\}.$ $Sz_e(G) = \sum_{uv \in E(G)} m_u(e G) m_v(e G),$
Padmakar–Ivan (e)	$PI_e(G) = \sum_{uv \in E(G)} (m_u(e G) + m_v(e G)),$
Geometric Mean-Szeged(e)	$SZ_e^{GM}(G) = \sum_{uv \in E(G)} \sqrt{m_u(e G)m_v(e G)}$
Sombor(VD)	$d_u = \sum_{v \subset V(G)} a_{uv}, SO(G) = \sum_{uv \in E(G)} \sqrt{d_u^2 + d_v^2}$
Scaled-Sombor(VD)	$SO^S(G) = \frac{1}{ E(G) } \sum_{uv \in E(G)} \sqrt{d_u^2 + d_v^2}$
RMS-Sombor(VD)	$SO^{RMS}(G) = \sqrt{\frac{1}{ E(G) } \sum_{uv \in E(G)} (d_u^2 + d_v^2)}$

Table 1. Cont.

Index	Expression
Somor(DD)	$\delta_u = \sum_v d(u, v), SO(G) = \sum_{uv \in E(G)} \sqrt{\delta_u^2 + \delta_v^2}$
Scaled-Sombor(DD)	$SO^S(G) = \frac{1}{ E(G) } \sum_{uv \in E(G)} \sqrt{\delta_u^2 + \delta_v^2}$
RMS-Sombor(DD)	$SORMS(G) = \sqrt{\frac{1}{ E(G) } \sum_{uv \in E(G)} (\delta_u^2 + \delta_v^2)}$
Randić Inverse Index	$RI = \sum_{uv \in E(G)} \sqrt{d_u d_v}, d_u = \sum_{v \in V(G)} a_{uv}$
Harmonic Index	$Harm = \sum_{uv \in E(G)} \frac{2}{d_u + d_v}$
Sum Connectivity Index	$SC = \sum_{uv \in E(G)} \sqrt{\frac{1}{d_u + d_v}}$
Hyper Zagreb	$HZ = \sum_{uv \in E(G)} (d_u + d_v)^2$
Geometric-Arithmetic	$GA = \sum_{uv \in E(G)} \frac{2\sqrt{d_u d_v}}{(d_u + d_v)}$
Symmetric Division Index	$SDD = \sum_{uv \in E(G)} \frac{(d_u^2 + d_v^2)}{d_u d_v}$
Cubic Vertex deg sum Index(Forgotten)	$F = \sum_{uv \in E(G)} (d_u^2 + d_v^2)$
Graph Energy	$GE = \sum_{i=1}^m  \lambda_i , m = 2^n, \lambda_i$ eigenvalue of A
Laplacian Energy	$GE = \sum_{i=1}^m  \lambda_i' , m = 2^n, \lambda_i'$ eigenvalue of $L = D - A, D =$ Diagonal vertex degree Matrix
Kirchhoff Index	$Kf(G) = \frac{1}{2} \sum_{\{i,j\} \subset V(G)} \Omega_{ij} = 2^n \sum_{i=1}^{m-1} 1/ \lambda_i' , \text{with } \lambda_m' = 0, m = 2^n, \Omega =$ Resistance Matrix
$\kappa$ : No. of spanning trees	$\kappa = \frac{(-1)^{m-1}}{m} c_{m-1}, c_{m-1}$ : coefficient of $\lambda^{l^2}$ in the Laplacian Polynomial.

<sup>a</sup> Mixed edge-vertex indices, total versions and entropies of indices are defined in ref. [41,42]; Geometric mean Szeged, Sombor-RMS, Sombor(scaled) and DD versions of these indices were introduced in [43].

There are a few spectral-based indices that we have computed in the present study. These are graph energies, Laplacian energies, Kirchhoff indices, the number of spanning trees and the corresponding spectral and Laplacian polynomials. These two polynomials are computed using author's codes [56–58] in quadruple precision arithmetic. The corresponding eigenvalues are also computed. As the order of the n-cube adjacency matrices increases as  $2^n \times 2^n$ , and thus the sizes of the matrices explode rapidly, we need to invoke some computational techniques for the robust numerical computations of the spectra and the characteristic polynomials so that we could go up to the 23-cube in this study. We have employed a fast recursive Hadamard transform method which was considered by the author in a few studies [59] including in a recent review [22]. Hence, we shall not repeat the details except stating that the Hadamard matrix transform was used recursively, which brings robustness to the numerical computations of spectra of the n-cubes. We did not use any prior mathematically known results or wreath product symmetry simplifications to factor the secular determinants in these numerical computations of the spectra of n-cubes up to  $n = 23$ . However, the spectra indeed form very nice patterns that can be readily cast into exact analytic expressions for the spectra of the n-cubes.

The matching polynomials of n-cubes were also computed in this study. As noted in the previous section, matching polynomials of such highly clustered structures have

been a topic of intense research as they pose a considerable computational challenge. We note that although the constant coefficients of the matching polynomials of the smaller  $n$ -cubes can be computed using algorithms that invoke computing the permanents of the adjacency matrices of hypercubes, the matching polynomial computations are considerably more challenging. We have modified the previously developed codes for matching polynomials [58,60] by introducing dynamic programming and storage of the computed characteristic polynomials of the line graphs and matching polynomials of cyclic graphs. The computed expressions for these polynomials are stored separately in a file and retrieved to memory as needed. We invoke recursive reduction algorithm to generate the matching polynomials of  $n$ -cubes. However, even with all such robust computational modifications all coefficients of the matching polynomials of the  $n$ -cubes could be computed only up to  $n = 6$ , demonstrating the computational and combinatorial complexity of the matching polynomial of the  $n$ -cube problem that seems to require more robust techniques in conjunction with artificial intelligence.

### 3. Results and Discussion

#### a. Topological Indices and Distance Degree Vector Sequences of $n$ -cubes

Hypercube graphs are arc-transitive and symmetric, possessing an automorphism group that is isomorphic with the wreath product group  $S_n[S_2]$  for  $Q_n$ , the  $n$ -cube graph. The order of the automorphism group is  $n! \times 2^n$ . Consequently, their properties tend to be both interesting and challenging due to the high degree of symmetry and arc-transitivity. The vertex degrees of  $Q_n$  are all the same and equal to  $n$ . Although this property can be used for analytical simplifications of various expressions, our numerical computations did not use these features as the codes are meant to be sufficiently general for any graph, whether vertex- or edge- or arc-transitive or not. Once the results are numerically obtained, they provide independent validations of the analytical expressions which are also obtained here for all topological indices using the degeneracies of vertex and distance degrees.

Table 2 shows the numerical results computed from the TopoChemie-2020 package [58] that takes the neighborhood information as the input to generate the distance matrices in  $r - 1$  iterations where  $r$  is the radius of the graph. Table 2 lists a number of vertex degree-based indices and several distance-based indices together the graph entropies for both the 11-dimensional and 12-dimensional hypercubes. As seen from Table 2, some of the topological indices such as the Randić index merely reduce to  $2^n - 1$  or the Mersenne number  $M_n$ , where  $n$  in this study shall always designate the dimension of the hypercube. Incidentally, the Mersenne numbers in the context of hypercubes and applications have been extensively studied by Carbó-Dorca and co-workers [1–5]. On the other hand, the geometric-arithmetic and the symmetric-division indices are directly related to the number of edges and twice the number of edges of the hypercube, respectively (Table 2). Some of the indices exhibit direct proportional relation; for example, the first and second Zagreb indices have a ratio of  $(n/2)$  for all  $n$ -cubes. The celebrated Wiener index is given by  $n2^{2(n-1)}$  in agreement with the previous results in the literature [46–51].

As seen from Table 2, several topological indices of the  $n$ -cube graphs are more complex compared to the purely vertex-degree-based indices. For example, the hyper-Wiener, Harary, ABC, Balaban and all distance-based indices such as the Szeged, Padmakar-Ivan, Sombor (DD and VD)-both vertex and edge versions as well as hyper-Zagreb, and augmented Zagreb indices exhibit more complex relations. Likewise, the Kirchhoff index as well as the spectral-based indices exhibit binomial distributions. We shall discuss the spectral-based indices separately in the next section. We have not shown the results of the Mostar indices of  $n$ -cubes because for such arc-transitive and symmetric graphs the Mostar indices go to zero, as these indices measure the degree of peripheral imperfections, and since hypercubes exhibit no such peripheral imperfections. Thus, their vertex and edge versions of Mostar indices go to zero.

**Table 2.** Numerical Results for various distance, degree-based Topological indices and entropies of 11-Cube and 12-Cube.

TI	11-Cube	12-Cube
No. of Edges	11,264	24,576
Wiener Index	11,534,336	50,331,648
Schultz Index	253,755,392	1,207,959,552
Hyper Wiener Index	$4.0370176 \times 10^7$	$1.8874368 \times 10^8$
$M_1$ (Zagreb-1)	247,808	589,824
$M_2$ (Zagreb-1)	1,362,944	3,538,944
Harary Index	1.0909090909090909	1.0833333333333333
RMS –Distance Index	183.82600468921692	282.6163477224911
Randić	1024	2048
Cubic Vertex deg sum Index	2,725,888	7,077,888
ABC	4579.467217918758	9605.971476119475
Balaban J index	1.2219570405729212	1.199882823942538
Szeged Index	$1.1811160064 \times 10^{10}$	$1.03079215104 \times 10^{11}$
Padmakar–Ivan Index(v)	23,068,672	100,663,296
Geometric-Mean Szeged	$1.1534336 \times 10^7$	$5.0331648 \times 10^7$
Szeged Index (e)	$2.952790016 \times 10^{11}$	$3.118146256896 \times 10^{12}$
Padmakar–Ivan Index (e)	115,343,360	553,648,128
Geometric-Mean Szeged (e)	$5.767168 \times 10^7$	$2.76824064 \times 10^8$
Szeged Index (ev)	$5.905580032 \times 10^{10}$	$5.66935683072 \times 10^{11}$
Mostar(ev)	46,137,344	226,492,416
Padmakar–Ivan Index (ev)	69,206,016	327,155,712
Geometric-Mean Szeged (ev)	$2.5791559371326845 \times 10^7$	$1.1803817749849734 \times 10^8$
Total Szeged Index	$4.25201762304 \times 10^{11}$	$4.355096838144 \times 10^{12}$
Total Padmakar–Ivan Index	276824064	4.4519388949849737E+8
Total Geometric-Mean Szeged	$9.499757537132685 \times 10^7$	$1.1803817749849734 \times 10^8$
Randić Inverse Index	123,904	294,912
Harmonic Index	1024	2048
Sum-Connectivity index	2401.4928690296374	5016.554993219602
Hyper-Zagreb	5,451,776	$1.4155776 \times 10^7$
Geometric-Arithmetic Index	11264	24,576
Symmetric-division Index	22,528	49,152
Augmented Zagreb	2,494,357.888000517	6,891,767.729528946
Sombor(VD)	175,226.7172323173	417,068.5501066585
Sombor(VD) <sup>s</sup>	15.556349186107717	16.97056274848057
Sombor(VD) <sup>RMS</sup>	15.556349186107717	16.97056274847714
Sombor(DD)	$1.7943215844589293 \times 10^8$	$8.541563906184366 \times 10^8$
Sombor(DD) <sup>s</sup>	15,929.701566574302	34,755.71250888821
Sombor(DD) <sup>RMS</sup>	15,929.701566570542	34,755.71250888118
All S (entropies)	9.3293670784	10.10952563595

Table 3 shows the exact analytical expressions for all of the topological indices that are included in the present study. The expressions were obtained in two different ways—one is through numerical interpolations of the computed results, and the second method is through the simplification and reduction in analytical expressions for these indices. As seen from Table 3, the expressions also provide us with how these indices vary with the order  $n$ , and order of the multiplicative powers of 2. These values also provide computational and combinatorial complexity measures of the various topological indices. A few trends can be seen from Table 3. For example, the Wiener index and vertex version of the Szeged index have a similar form except the power factor being  $2(n - 1)$  for the Wiener index, while it is  $3(n - 1)$  for the Szeged index. Consequently, the geometric mean Szeged index introduced by the author [43] becomes identical to the Wiener index for  $n$ -cubes. Likewise, the Gutman index and the second Zagreb index bear a similar relation to that of the Wiener and Szeged indices. The edge versions of all indices exhibit more complex relations compared to the vertex versions of the same indices. The scaled and geometric means of both vertex degree and distance degree versions become identical to one other (see Table 3). We note that the mixed edge-vertex versions of all indices are quite different from their vertex or edge counterparts; a conspicuous case being that of the Mostar index, which is zero for the pure version but becomes nonzero for the mixed edge-vertex version (see Table 3). Moreover, the expressions for the Balaban and Harary indices of  $n$ -cubes are considerably more complex (Table 3).

**Table 3.** Analytical expressions for various distance, degree-based Topological indices and entropies of  $nD$ -hypercube.

TI	Expression
Wiener	$n2^{2(n-1)}$
Schultz	$n^2 2^{2n-1}$
Gutman	$n^3 2^{2(n-1)}$
Hyper-Wiener	$\frac{n(n+3)}{4} 2^{2(n-1)}$
$M_1$ (Zagreb-1)	$n^2 2^n$
$M_2$ (Zagreb-1)	$n^3 2^{n-1}$
Harary Index	$2^{n-1} \sum_{j=1}^n \binom{n}{j} \frac{1}{j}$
Randić	$2^n - 1 = M_n$
ABC	$2^n \sqrt{\frac{2^n - 1}{2}}$
Balaban J index	$J = \frac{n \cdot 2^n}{2^{n-1}(n-2)+2}$
Harmonic Index	$H = 2^{(n-1)}$
Sum-Connectivity index	$\sqrt{\frac{n}{2}} 2^{n-1}$
Hyper-Zagreb	$4n^3 2^{(n-1)}$
Geometric-Arithmetic Index	$n2^{(n-1)}$
Symmetric-division Index	$n2^n$
Augmented Zagreb	$\frac{2^{n-4} n^7}{(n-1)^3}$
Sombor(VD)	$\sqrt{2} n^2 2^{(n-1)}$
Sombor(VD) <sup>s</sup>	$\sqrt{2} n$
Sombor(VD) <sup>RMS</sup>	$\sqrt{2} n$
Sombor(DD)	$\sqrt{2} n^2 2^{(n-1)}$

**Table 3.** *Cont.*

TI	Expression
Sombor(DD) <sup>s</sup>	$\sqrt{2}n2^{(n-1)}$
Sombor(DD) <sup>RMS</sup>	$\sqrt{2}n2^{(n-1)}$
Cubic Vertex deg sum Index	$n^32^n$
Padmakar–Ivan <sub>v</sub>	$n 2^{2n-1}$
Szeged <sub>v</sub>	$n 2^{3(n-1)}$
Szeged <sub>v</sub> <sup>GM</sup>	$n2^{2(n-1)}$
Padmakar–Ivan <sub>e</sub>	$\binom{n}{2}2^{2n-1}$
Szeged <sub>e</sub>	$n(n-1)^22^{3n-5}$
Szeged <sub>e</sub> <sup>GM</sup>	$\binom{n}{2}2^{2(n-1)}$
Padmakar–Ivan <sub>ev</sub>	$\frac{n(n+1)}{2}2^{2(n-1)}$
Szeged <sub>ev</sub>	$\binom{n}{2}2^{3(n-1)}$
MO <sub>ev</sub>	$n(n-3)2^{2n-3}$
Aug-Zagreb	$\frac{n^7}{(n-1)^3}2^{(n-4)}$
S (entropies)	$\ln(n) + (n-1)\ln 2$
Kirchhoff Index	$2^n \sum_{j=2}^n \binom{n}{j-1} \frac{1}{2^{j-1}}$
Graph Energy	$\frac{4 \prod_{j=1}^{n/2} (n-j)}{[(\frac{n-2}{2})!]}, n \text{ even}$ $(n+1) \frac{\prod_{j=0}^{(n+1)/2} (n-j+1)}{2(\frac{n-1}{2})!}, n \text{ odd}$
Characteristic Polynomial	$(x+n)(x+n-2)^{n1}(x+n-4)^{n2} \dots \dots (x-n),$ $n_k = \binom{n}{k}$
Laplacian Polynomial	$x(x-2)^{n1}(x-4)^{n2} \dots \dots (x-2n),$ $n_k = \binom{n}{k}$
No of spanning trees $\kappa$	$\frac{1}{2^n} \prod_{j=1}^n \binom{n}{j} 2^j$
Laplacian Energy (scaled)	$\frac{1}{2^n} \sum_{j=1}^n \binom{n}{j} 2^j$

Analytical expressions for four of the topological indices that we have derived in Table 3 have been obtained before by a number of authors [46–51]. The most recent work on the topological indices of n-cubes is that of Kaatz and Bultheel [51]. As noted by these authors [51], the exact analytical expressions have been obtained previously for the Wiener index, Szeged index(vertex), Balaban and Kirchhoff indices [46–50]. The expressions that are listed in Table 2 of ref. [51] match with our results in Table 3 of the current work. Furthermore, the numerical results for these indices that are listed in Table 3 of ref. [51] agree with our computed results for these indices. In Table 2 of the present study we have compiled a more exhaustive set of results for several other indices that have not been obtained in previous studies for the n-cubes, with the exception of four indices that we have already mentioned.

As seen from Table 3, all entropies derived from the various topological indices for the  $n$ -cube reduce to the same expression:

$$S = \ln(n) + (n - 1)\ln 2$$

We have validated this entropy behavior with our codes, and we find that all entropies derived from the topological indices listed in Tables 1 and 2 reduce to the above expression. This is an interesting feature of  $n$ -cubes, and it is a clear and direct consequence of the arc-transitive nature of hypercubes resulting in degenerate vertex and distance degrees.

Following Quintas and coworkers [61], the Distance Degree Sequence Vector (DDSV) is defined as a  $p$ -tuple vector  $(d_{i0}, d_{i1}, d_{i2}, \dots, d_{ij}, \dots, d_{ip})$  where  $d_{ij}$  is the number of vertices at distance  $j$  from a vertex  $v_i$  of the  $n$ -cube. Consequently, by computing the number of vertices at a given distance from the vertex  $v_i$ , we can associate a DDSV for that vertex of the  $n$ -cube. We compute the DDSVs of vertices of  $n$ -cubes using the distance matrix that we have previously generated for the computations of topological indices, and as described earlier for the  $n$ -cube the algorithm computes the distance matrix in  $n - 1$  iterations using the TopoChemie-2020 package [58]. As the  $n$ -cube is an arc-transitive and symmetric graph, the DDSVs of all vertices become identical, and moreover the DDSV of each vertex exhibits a symmetric binomial sequence as illustrated in Figure 2 for a hypercube of dimension 108. As can be seen from Figure 2, the DDSVs of hypercubes exhibit a symmetric binomial distribution, a result which was not known up to now.

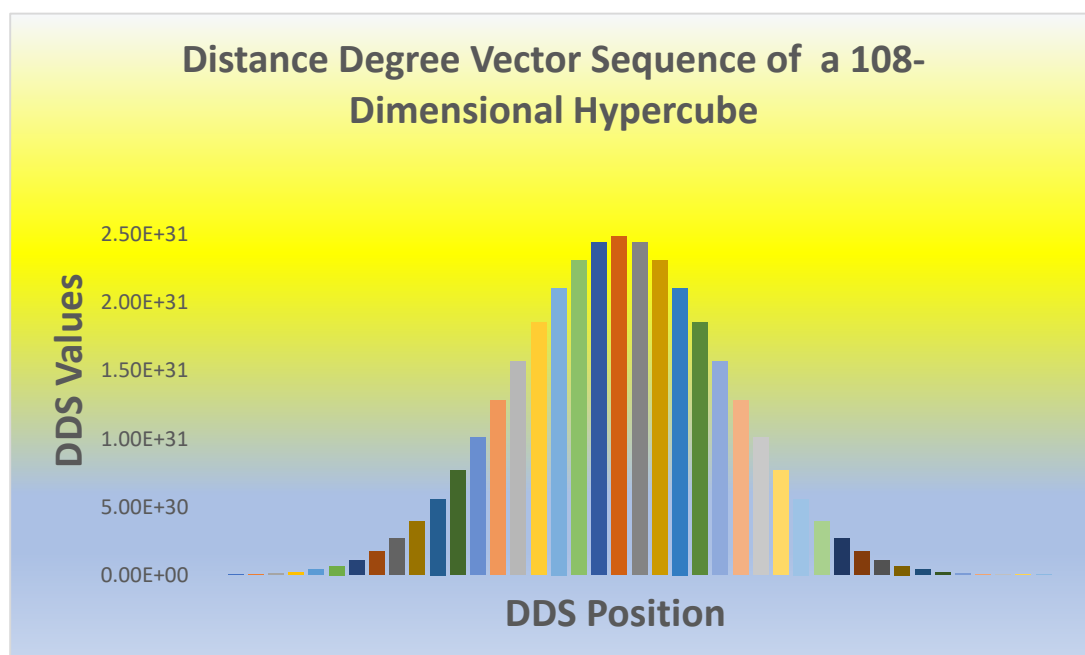


**Figure 2.** Distance Degree Vector Sequence of a 108-Dimensional hypercube.

#### b. Spectral properties

Next, we consider the spectra of the  $n$ -cubes, the corresponding Laplacian spectra as well as the corresponding spectral polynomials. As the adjacency matrix of the  $n$ -cube is of order  $2^n \times 2^n$ , the sizes of both adjacency and Laplacian matrices grow rapidly; for example, for a 23-cube the matrix is of order  $8,388,608 \times 8,388,608$ . Consequently, numerical computations of *all* eigenvalues of these matrices can be computationally daunting without explicitly invoking the hyperoctahedral symmetry group of the hypercubes. Alternatively, we have shown previously that orthogonal Hadamard matrices can be of significant use in simplifying the eigenvalue problem of such large matrices [22,59]. Collado [62] has also made use of the Hadamard transform technique for extracting the eigenvalues of the adjacency matrices of large carbon nanotubes.

In the case of n-cube graphs, we have invoked a recursive application of the Hadamard matrix orthogonal transform for the rapid numerical computations of the spectra of n-cubes. The techniques facilitate elegant computations of the spectra of up to the 23-cube numerically without any prior assumption of known factorizations of the characteristic polynomials of n-cubes. In this method, we orthogonally rotate the adjacency matrix of the n-cube recursively, resulting in great numerical simplifications. Table 4 shows the numerical results thus obtained for all hypercubes up to dimension 23. The limitation of dimension 23 has to do with the DRAM limitations, and larger n-cubes can be handled on systems equipped with greater DRAMs such as workstations and supercomputers. As expected, due to the wreath product automorphism group of the n-cubes, the spectral patterns exhibit a high degree of degeneracy (Table 4). The numbers in parenthesis are the frequencies of a given eigenvalue that occur in the spectra of hypercubes. Based on the observation of the numerical results in Table 4 and the use of mathematical induction, we deduce the binomial distribution of the eigenvalues as displayed in Figure 3 for the computed spectral distribution of the 23-cube.

**Table 4.** Computed Spectra of nD-hypercubes (up to n = 23) using Recursive Hadamard Transform <sup>a</sup>.

n	Spectra	Graph Energy
8	−8 (1) −6 (8) −4 (28) −2 (56) 0 (70) 2 (56) 4 (28) 6 (8) 8 (1)	560
9	−9 (1) −7 (9) −5 (36) −3 (84) −1 (126) 1 (126) 3 (84) 5 (36) 7 (9) 9 (1)	1260
10	−10 (1) −8 (10) −6 (45) −4 (120) −2 (210) 0 (252) 2 (210) 4 (120) 6 (45) 8 (10) 10 (1)	2520
11	−11 (1) −9 (11) −7 (55) −5 (165) −3 (330) −1 (462) 1 (462) 3 (330) 5 (165) 7 (55) 9 (11) 11 (1)	5544
12	−12 (1) −10 (12) −8 (66) −6 (220) −4 (495) −2 (792) 0 (924) 2 (792) 4 (495) 6 (220) 8 (66) 10 (12) 12 (1)	11,088
13	−13 (1) −11 (13) −9 (78) −7 (286) −5 (715) −3 (1287) −1 (1716) 1 (1716) 3 (1287) 5 (715) 7 (286) 9 (78) 11 (13) 13 (1)	24,024
14	−14 (1) −12 (14) −10 (91) −8 (364) −6 (1001) −4 (2002) −2 (3003) 0 (3432) 2 (3003) 4 (2002) 6 (1001) 8 (364) 10 (91) 12 (14) 14 (1)	48,048
15	−15 (1) −13 (15) −11 (105) −9 (455) −7 (1365) −5 (3003) −3 (5005) −1 (6435) 1 (6435) 3 (5005) 5 (3003) 7 (1365) 9 (455) 11 (105) 13 (15) 15 (1)	102,960
16	−16 (1) −14 (16) −12 (120) −10 (560) −8 (1820) −6 (4368) −4 (8008) −2 (11,440) 0 (12,870) 2 (11,440) 4 (8008) 6 (4368) 8 (1820) 10 (560) 12 (120) 14 (16) 16 (1)	205,920
17	−17 (1) −15 (17) −13 (136) −11 (680) −9 (2380) −7 (6188) −5 (12376) −3 (19,448) −1 (24,310) 1 (24,310) 3 (19,448) 5 (12,376) 7 (6188) 9 (2380) 11 (680) 13 (136) 15 (17) 17 (1)	437,580
18	−18 (1) −16 (18) −14 (153) −12 (816) −10 (3060) −8 (8568) −6 (18,564) −4 (31,824) −2 (43,758) 0 (48,620) 2 (43,758) 4 (31,824) 6 (18,564) 8 (8568) 10 (3060) 12 (816) 14 (153) 16 (18) 18 (1)	875,160
19	−19 (1) −17 (19) −15 (171) −13 (969) −11 (3876) −9 (11,628) −7 (27,132) −5 (50,388) −3 (75,582) −1 (92,378) 1 (92,378) 3 (75,582) 5 (50,388) 7 (27,132) 9 (11,628) 11 (3876) 13 (969) 15 (171) 17 (19) 19 (1)	1,847,560
20	−20 (1) −18 (20) −16 (190) −14 (1140) −12 (4845) −10 (15,504) −8 (38,760) −6 (77,520) −4 (125,970) −2 (167,960) 0 (184,756) 2 (167,960) 4 (125,970) 6 (77,520) 8 (38,760) 10 (15,504) 12 (4845) 14 (1140) 16 (190) 18 (20) 20(1)	3,695,120
21	−21 (1) −19 (21) −17 (210) −15 (1330) −13 (5985) −11 (20,349) −9 (54,264) −7 (116,280) −5 (203,490) −3(293,930) −1 (352,716) 1 (352,716) 3 (293,930) 5 (203,490) 7 (116,280) 9 (54,264) 11 (20,349) 13 (5985) 15 (1330) 17 (210) 19 (21) 21 (1)	7,759,752
22	−22 (1) −20 (22) −18 (231) −16 (1540) −14 (7315) −12 (26,334) −10 (74,613) −8 (170,544) −6 (319,770) −4 (497,420) −2 (646,646) 0 (705,432) 2 (646,646) 4 (497,420) 6 (319,770) 8 (170,544) 10 (74,613) 12 (26,334) 14 (7315) 16 (1540) 18 (231) 20 (22) 22 (1)	15,519,504
23	−23 (1) −21 (23) −19 (253) −17 (1771) −15 (8855) −13 (33,649) −11 (100,947) −9 (245,157) −7 (490,314) −5 (817,190) −3 (1,144,066) −1 (1,352,078) 1 (1,352,078) 3 (1,144,066) 5 (817,190) 7 (490,314) 9 (245,157) 11 (100,947) 13 (33,649) 15 (8855) 17 (1771) 19 (253) 21 (23) 23 (1)	32,449,872

<sup>a</sup> The corresponding Laplacian spectra are obtained by right-shifting the spectra by n. Numbers in parenthesis are the frequencies of the eigenvalue.

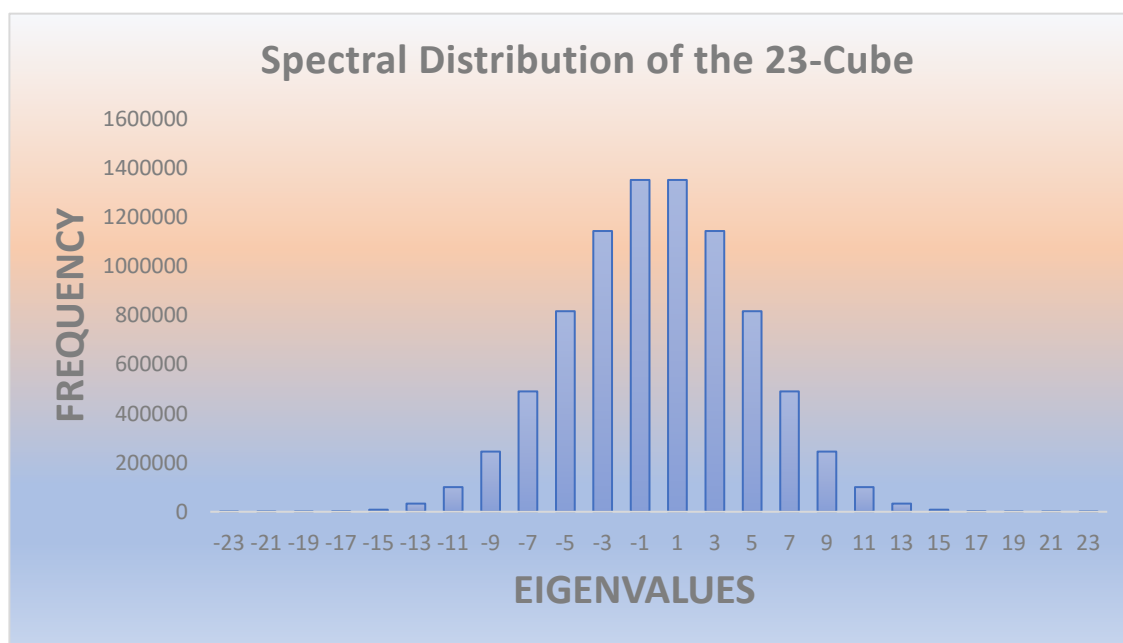


**Figure 3.** Spectral Distribution of a 23-Dimensional hypercube; the corresponding Laplacian Spectra are obtained by right-shifting the  $x$ -axis values by 23.

Both numerical induction and analytical techniques based on factoring the characteristic polynomial of the  $n$ -cube result in the spectral pattern and the characteristic polynomial that are shown in Table 3. The corresponding Laplacian spectra are readily obtained by right-shifting the adjacency spectra by  $n$  for an  $n$ -cube, which results in the lowest eigenvalues of the Laplacian matrix being 0, as expected. The graph and Laplacian energies can be readily obtained from the spectra using the expressions shown in Table 1 for the graph energy. We note that the topic of graph energies of several clustered graphs including hypercubes has received considerable attention, as seen from the latest work of Diudea et al. [52]. The graph and Laplacian energies of hypercubes are shown in Table 3, and our computed numerical results for the graph energies as well as the binomial spectral distribution are fully consistent with the previous works [50–52].

The Laplacian spectra and the Laplacian polynomials of  $nd$ -hypercubes facilitate the computations of the Kirchhoff indices and the number of spanning trees of the hypercubes. The Kirchhoff indices have been the topic of several studies [44,45] owing to their importance in resistance matrices and resistance distances. The Kirchhoff index, which is an inverse analog of the Wiener index, was originally defined in terms of the resistance distances [44,45], but the Kirchhoff index can be computed using the Laplacian spectra with the expression shown in Table 1. The result thus obtained for the Kirchhoff index is shown in Table 3. Another important result that can be derived from the Laplacian polynomial is that the scaled coefficient of  $\lambda^2$  term in the Laplacian polynomial yields the number of spanning trees (Table 1). The computed numerical results of the number of spanning trees of the hypercubes are shown in Table 5 together with the  $\log$ (to the base 10) values of the number of spanning trees. As seen from Table 5, the numbers of spanning trees of  $n$ -cubes grow in astronomical proportions as a function of  $n$ , revealing the combinatorial complexity of the  $n$ -cubes.

**Table 5.** Combinatorial Enumeration of spanning trees of nD-hypercube.

n	$\kappa$	$\log(\kappa)$
3	384	2.584331224368
4	42,467,328	7.628054936494
5	20,776,019,874,734,407,680	19.317562352076
6	$1.6575091270477789938706015460369005145 \times 10^{45}$	45.219455928519
7	$1.5385084434981466048710053999438123881 \times 10^{101}$	101.187099884044
8	$1.740475945846247472883023392740201058 \times 10^{220}$	220.240668025518
9	$6.798128703006646365181450760022537757 \times 10^{470}$	470.832389382441
10	$2.100521551103851822257498283042967383 \times 10^{994}$	994.322327141707
11	$5.0754732540292453608181958787281340906 \times 10^{2081}$	2081.705476543537
12	$2.583802660235773447053323186483352567 \times 10^{4330}$	4330.412259341040

c. Matching Polynomials

The matching polynomial of an n-cube enumerates the number of ways to place k-dimers on an n-cube comprising of  $n \times 2^{n-1}$  edges such that no two dimers share the same vertex. Symbolically, it is defined by  $M(x)$  for an n-cube as:

$$M(x) = \sum_{k=0}^m (-1)^k M_k x^{2m-2k}, \quad m = 2^{n-1} \text{ for an } n \text{ - cube}$$

The constant coefficient of the matching polynomial or  $M_{2^{n-1}}$  in the above expression corresponds to the case when all the vertices are covered by the dimers or the number of disjoint dimers placed is the Mersenne number,  $2^{n-1}$ , thus resulting in a perfect matching. Combinatorial enumeration of the perfect matchings of the n-cube has been a long-standing open-ended problem, and hence it has been a subject of several investigations [53,54] since the pioneering work of Graham and Harary [53]. Graham and Harary [53] have obtained the number of perfect matching of hypercubes with  $n \leq 5$  by obtaining the permanents of their adjacency matrices, and in particular, they enumerate the number of perfect matchings of the 5-cube as 589,185. In the most recent work on the topic, Östergård and Pettersson [54] have employed a dynamic programming technique analogous to the one used in the present study. The number of perfect matchings of the 6-cube [70] and 7-cube [54] are 16,332,454,526,976 and 391,689,748,492, 473, 664,721, 077,609,089, respectively. It is thus readily seen that the problem of computing the matching polynomials of n-cubes is computationally and combinatorially far more complex than computing the constant term of the matching polynomial, which itself grows astronomically. Hosoya as well as the author and Hosoya [63–67] have proposed computational techniques for selective labelling of some of the edges of such graphs with imaginary weights in order to generate the matching polynomials from the characteristic polynomials of the imaginary-weighted adjacency matrices. The technique is extremely useful when such an edge-weighted graph can be found, as it simplifies the matching polynomial problem into an  $O(n^3)$  problem since the characteristic polynomial can be obtained by the present author’s codes and techniques [56–58] by  $O(n^3)$  computations using  $n$  iterative computations of traces of matrices generated through matrix multiplication methods. Hosoya and the author [66,67] applied such a technique to generate the matching polynomial of a 3-cube from the characteristic polynomial of the associated edge-weighted cube with selected edges weighted with imaginary weights. However, the technique is not general and it is not always feasible to find such edge-weighted graphs for all n-cubes. At present we are not aware of any such algorithm to find edge-weighted n-cubes whose characteristic polynomials yield the matching polynomials of n-cubes.

As described in the previous section, we have made significant enhancements through dynamic programming and reducing repeated computations of matching polynomials of line graphs and cyclic graphs by previous computations, and storing these polynomials

in a sequential binary file. In the process of recursive computation and reduction techniques numerous fragment graphs are generated in the reductive algorithm, which are trees, line graphs and cyclic graphs with pendants of varied complexities. In the present dynamic programming method, the matching polynomials are not repeatedly computed for such fragments, as they are read from the stored files and brought into the computer’s memory as needed. The techniques definitely reduce the computational complexity of the matching polynomial problem, and thus we show the computed matching polynomials of the 4-cube, 5-cube and 6-cube in Tables 6–8, respectively. As seen from these tables, the nonzero coefficients of the matching polynomials of terms beyond the third term grow in astronomical proportions. As special cases of our computations, the constant coefficient in the matching polynomial of the 5-cube agrees with Graham and Harary’s result [53], while for the 6-cube our computed result is in accord with the results listed in Refs. [54,69], thus providing a validation of the computed results in Tables 6–8. Furthermore, the numerical results in Tables 6–8 obtained using our enhanced computer codes match with the online encyclopaedia sequence A192437 attributed to an unpublished work of D. H. Wiedemann and other works that are listed in reference [70].

**Table 6.** Matching Polynomial of the 4-Cube <sup>a</sup>.

k	M <sub>k</sub>
0	1
1	−32 (n × 2 <sup>n−1</sup> )
2	400 (25/2) × M <sub>1</sub>
3	−2496
4	8256
5	−14,208
6	11,648
7	−3712
8	272(17 × 2 <sup>4</sup> )

<sup>a</sup> k refers to the number of disjoint dimers, as defined in the matching polynomial:  $M(x) = \sum_{k=0}^m (-1)^k M_k x^{2m-2k}$ ,  $m = 2^{n-1}$ , Mersenne number for an n-cube.

**Table 7.** Matching Polynomial of the 5-Cube.

k	M <sub>k</sub>
0	1
1	−80 (n × 2 <sup>n−1</sup> )
2	2840(71/2) × M <sub>1</sub>
3	−59,120
4	803,580
5	−7,517,264
6	49,715,240
7	−235,146,480
8	795,862,790
9	−1,910,146,160
10	3,190,117,800
11	−3,594,554,960
12	2,605,908,220
13	−1,129,177,840

**Table 7.** *Cont.*

<b>k</b>	<b>M<sub>k</sub></b>
14	259,084,440
15	−25,108,944
16	589,185(3 <sup>2</sup> × 5 × 13,093)

**Table 8.** Matching Polynomial of the 6-Cube.

<b>k</b>	<b>M<sub>k</sub></b>
0	1
1	−192 (n × 2 <sup>n−1</sup> )
2	17,376 (181/2) × M <sub>1</sub>
3	−986,240
4	39,408,480
5	−1,179,696,384
6	27,488,385,408
7	−511,416,198,144
8	7,732,531,647,360
9	−96,216,012,236,800
10	994,137,263,758,848
11	−8,583,228,570,909,696
12	62,184,244,929,659,648
13	−378,969,619,199,569,920
14	1,944,655,398,731,796,480
15	−8,398,980,067,449,999,360
16	30,480,925,212,093,104,640
17	−92,675,048,634,081,607,680
18	235,053,748,112,782,356,480
19	−494,482,501,391,128,289,280
20	856,482,708,316,893,954,048
21	−1,210,188,907,641,505,775,616
22	1,378,948,882,982,541,631,488
23	−1249,011,213,103,104,491,520
24	883,258,965,992,225,095,680
25	−476,635,207,372,408,553,472
26	190,551,239,146,197,909,504
27	−54,258,655,709,480,353,792
28	10,420,946,627,414,016,000
29	−1,246,585,402,333,593,600
30	81,808,261,704,974,336
31	−2,333,280,165,691,392
32	16,332,454,526,976 2 <sup>15</sup> × 3 <sup>2</sup> × 7 × 7,911,539

We have noted a few trends from the numerical results for the various coefficients in the matching polynomials of the n-cubes reported in Tables 5–8. First, the third nonzero coefficient in the matching polynomial is a rational multiple of the second coefficient in the polynomial that is given by  $n \times 2^{n-1}$ . We note that the third (nonzero) coefficient ( $M_2$ ) in the matching polynomials of the n-cube forms an interesting sequence in terms of its previous (nonzero) coefficient ( $M_1$ ):

$$\{(1/2)M_1, (7/2)M_1, (25/2)M_1, (71/2) M_1, (181/2)M_1, (435/2)M_1, (1009/2)M_1, (2287/2)M_1\dots\}$$

for the 2-cube, 3-cube, 4-cube, 5-cube, 6-cube, 7-cube, 8-cube, and 9-cube, respectively (Tables 5–8 show up to the 6-cube). Hence we have a new integer sequence: {1, 7, 25, 71, 181, 435, 1009, 2287, ...}. The prime factors of the constant coefficients exhibit complex patterns in that they are:

$$\{1, 2, 3^2, 17 \times 2^4, 3^2 \times 5 \times 13, 093, 2^{15} \times 3^2 \times 7 \times 7, 911, 539\dots\}$$

for the  $K_2$  graph, 2-cube, 3-cube, 4-cube, 5-cube and 6-cube, respectively. Some powers of 2 appear as factors only for even n-cubes, and some powers of 3 appear to be a factor for the constant coefficients of odd n-cubes including the possibility of 3 being a divisor. In fact, the number of perfect matchings of the 7-cube, 391,689,748,492,473,664,721, 077,609,089, is divisible by 3 but not by 9. The corresponding constant coefficient has been previously obtained for the 3-cube as 9 [66], and the matching polynomial of the 3-cube [66] is given by:

$$M(3\text{-cube}) = x^8 - 12 x^6 + 42 x^4 - 44 x^2 + 9$$

We note that the third coefficient is (7/2) times the second coefficient for the cube, a trend that we have noted above. The above matching polynomial of the 3-cube was obtained by assigning imaginary weights to three of the edges of the cube, each edge separated by one edge in the direction of arrows. Subsequently, the rows of the adjacency matrix need to be rearranged in the order of odd vertex labels first followed by even vertex labels. The secular determinant of such a complex but hermitian matrix yields the matching polynomial of the cube. We have made several such trial attempts to compute the matching polynomial of the 4-cube, but thus far we were unable to find a suitable edge-weighted graph that would generate the matching polynomial of the 4-cube through the secular determinant method. The recursive procedures that we have used for computing the matching polynomials are extremely intensive and do not work well beyond the 6-cube. Consequently, we envisage a combination of recursive reduction and artificial intelligence techniques to speed up the recursive pruning and computations, so that when sufficiently larger cluster graphs such as cubes and cubes with pending bonds are reached the technique can stop the recursive reduction. In this case the matching polynomials of such cluster fragments need to be stored in a library, and then using prior methods and machine learning techniques the matching polynomials of the parent graph can be computed. Unlike the spectral polynomials, at present, no relations seem to exist between the matching polynomial of the n-cube and the matching polynomials of the (n-1)-cube, (n-2)-cube, (n-3)-cube ... , 3-cube. If such relations can be found then the matching polynomials of n-cubes can indeed be computed more efficiently than the presently available methods to compute them. The other alternative is to find the complex-edge-weight n-cube whose characteristic polynomial is the matching polynomial of the n-cube.

#### 4. Conclusions

In the present work we have computed a large number of distance- and degree-based topological indices, entropies, spectra, the characteristic, and matching polynomials of n-dimensional hypercubes. We have demonstrated the power of recursive Hadamard transforms in computing the spectra of n-cubes. We have reported numerical results for several topological indices of 11- and 12-cubes and the numerical spectra of up to 23-cubes. The computed numerical results form the basis to validate the exact analytical expressions that we have obtained for the topological indices, spectra, and their polynomials. Furthermore, a robust dynamic programming technique was employed to compute the matching polynomials of nD-hypercubes. We have shown that both the computed distance degree vector sequences and spectra up to 108-cubes exhibit a binomial distribution. We note that the computations of the matching polynomials continue to pose computational challenges for such large highly clustered graphs, and future studies are desirable to combine recursive computing with machine learning and artificial intelligence techniques for robust computations of the matching polynomials of such highly clustered structures, including n-cubes for  $n \geq 7$ . At present only the

constant coefficient (391,689,748,492,473,664,721, 077,609,089) and the first three coefficients (1, -448, 97,440) of the matching polynomial of the 7-cube are known. The first 3 coefficients in the matching polynomials of the 8-cube and 9-cube are computed as (1, -1024, 516,608) and (1, -2304, 2,634,624), respectively. It is hoped that the present study will stimulate future works on these open-ended problems pertinent to the n-cubes.

**Funding:** This research received no external funding.

**Institutional Review Board Statement:** Not applicable.

**Informed Consent Statement:** Not applicable.

**Data Availability Statement:** All the data used in the manuscript are contained in the manuscript.

**Conflicts of Interest:** The author declares no conflict of interest.

## References

1. Carbó-Dorca, R. Boolean Hypercubes: The Origin of a Tagged Recursive Logic and the Limits of Artificial Intelligence. *Universal J. Math. Appl.* **2020**, *4*, 41–49. [[CrossRef](#)]
2. Carbó-Dorca, R.; Chakraborty, T. Divagations about the periodic table: Boolean hypercube and quantum similarity connections. *J. Comput. Chem.* **2019**, *40*, 2653–2663. [[CrossRef](#)] [[PubMed](#)]
3. Carbó-Dorca, R. Boolean hypercubes and the Structure of Vector Spaces. *J. Math. Sci. Model.* **2018**, *1*, 1–14. [[CrossRef](#)]
4. Carbó-Dorca, R. DNA unnatural base pairs and hypercubes. *J. Math Chem.* **2018**, *56*, 1353–1536. [[CrossRef](#)]
5. Carbó-Dorca, R. Natural Vector Spaces (inward power and Minkowski norm of a Natural Vector, Natural Boolean Hypercubes) and a Fermat's Last Theorem conjecture. *J. Math Chem.* **2017**, *55*, 914–940. [[CrossRef](#)]
6. Stanley, K.O.; D'Ambrosio, D.B.; Gauci, J. A hypercube-based encoding for evolving large-scale neural networks. *Artif. Life* **2009**, *15*, 185–212. [[CrossRef](#)]
7. Mezey, P.G. Similarity Analysis in two and three dimensions using lattice animals and ploycubes. *J. Math. Chem.* **1992**, *11*, 27–45. [[CrossRef](#)]
8. Fralov, A.; Jako, E.; Mezey, P.G. Logical Models for Molecular Shapes and Families. *J. Math. Chem.* **2001**, *30*, 389–409. [[CrossRef](#)]
9. Mezey, P.G. Some Dimension Problems in Molecular Databases. *J. Math. Chem.* **2009**, *45*, 1. [[CrossRef](#)]
10. Mezey, P.G. Shape Similarity measures for Molecular Bodies: A Three-dimensional Topological Approach in Quantitative Shape-activity Relation. *J. Chem. Inf. Comput. Sci.* **1992**, *32*, 650. [[CrossRef](#)]
11. Carbó-Dorca, R. Cantor-like transfinite sequences and Gödel-like incompleteness revealed by means of Mersenne transfinite dimensional boolean hypercube concatenation. *J. Math. Chem.* **2020**, *58*, 1–5. [[CrossRef](#)]
12. Balasubramanian, K. Combinatorial and quantum techniques for large data sets: Hypercubes and halocarbons. In *Big Data Analytics in Chemoinformatics and Bioinformatics*; Basak, S.C., Vračko, M., Eds.; Elsevier: Amsterdam, The Netherlands, 2023; pp. 187–218. ISBN 978-0-323-85713-0.
13. Gowen, A.A.; O'Donnella, C.P.; Cullenb, P.J.; Bell, S.E.J. Recent applications of chemical imaging to pharmaceutical process monitoring and quality control. *European. J. Pharm. Biopharm.* **2008**, *69*, 10–22. [[CrossRef](#)] [[PubMed](#)]
14. Bhaniramka, P.; Wenger, R.; Crawfis, R. Isosurfacing in higher Dimension. In Proceedings of the IEEE Visualization 2000. VIS 2000 (Cat. No. 00CH37145), Salt Lake City, UT, USA, 8–13 October 2000; pp. 267–270. [[CrossRef](#)]
15. Banks, D.C.; Linton, S.A.; Stockmeyer, P.K. Counting Cases in Substotope Algorithms. *IEEE Trans. Vis. Comput. Graph.* **2004**, *10*, 371–384. [[CrossRef](#)] [[PubMed](#)]
16. Liu, M.; Bassler, K.E. Finite size effects and symmetry breaking in the evolution of networks of competing Boolean nodes. *J. Phys. A Math. Theor.* **2010**, *44*, 045101. [[CrossRef](#)]
17. Wallace, R. Spontaneous symmetry breaking in a non-rigid molecule approach to intrinsically disordered proteins. *Molecular BioSyst.* **2012**, *8*, 374–377. [[CrossRef](#)]
18. Wallace, R. Tools for the Future: Hidden Symmetries. In *Computational Psychiatry*; Springer: Cham, Switzerland, 2017; pp. 153–165.
19. Wallace, R. Multifunction moonlighting and intrinsically disordered proteins: Information catalysis, non-rigid molecule symmetries and the 'logic gate' spectrum. *C. R. Chim.* **2011**, *14*, 1117–1121. [[CrossRef](#)]
20. Nandini, G.K.; Rajan, R.S.; Shantrinal, A.A.; Rajalaxmi, T.M.; Rajasingh, I.; Balasubramanian, K. Topological and Thermodynamic Entropy Measures for COVID-19 Pandemic through Graph Theory. *Symmetry* **2020**, *12*, 1992. [[CrossRef](#)]
21. Forster, P.; Forster, L.; Renfrew, C.; Forster, M. Phylogenetic network analysis of SARS-CoV-2 genomes. *Proc. Natl. Acad. Sci. USA* **2020**, *117*, 9241–9243. [[CrossRef](#)]
22. Balasubramanian, K. Symmetry, Combinatorics, Artificial Intelligence, Music and Spectroscopy. *Symmetry* **2021**, *13*, 1850. [[CrossRef](#)]
23. Darafsheh, M.R.; Ashrafi, A.R.; Darafsheh, A. The full non-rigid group of hexamethylbenzene using wreath product. *Chem. Phys. Lett.* **2006**, *421*, 566–570. [[CrossRef](#)]
24. Darafsheh, M.R.; Ashrafi, A.R.; Darafsheh, A. Computing the full nonrigid group of tetra-tert-butyltetrahedrane using wreath product. *Int. J. Quant. Chem.* **2005**, *105*, 485–492. [[CrossRef](#)]

25. Dabirian, M.; Iranmanesh, A. Nonrigid Group Theory of Water Clusters (Cyclic Forms): $(H_2O)_n$  for  $n = 2, 3, 4, 5$ . *Iran. J. Math. Sci. Inf.* **2008**, *3*, 13–30.
26. Temme, F.P. Time-reversal-based  $SU(2) \times S_n$  scalar invariants as (Lie Algebraic) group measures: A structured overview of generalized democratic-recoupled, uniform non-Abelian  $[AX]_n$  NMR spin systems, as abstract  $S_n \supset \cap S_{n-1} / U_n \supset \cap U_{n-1}$  chain networks. *J. Mag. Res.* **2004**, *167*, 119–132. [[CrossRef](#)] [[PubMed](#)]
27. Balasubramanian, K. Enumeration of internal rotation reactions and their reaction graphs. *Theor. Chim. Acta* **1979**, *53*, 129–146. [[CrossRef](#)]
28. Balasubramanian, K. Relativistic double group spinor representations of nonrigid molecules. *J. Chem. Phys.* **2004**, *120*, 5524–5535. [[CrossRef](#)] [[PubMed](#)]
29. Balasubramanian, K. Character tables of  $n$ -dimensional hyperoctahedral groups and their applications. *Mol. Phys.* **2016**, *114*, 1619–1633. [[CrossRef](#)]
30. Balasubramanian, K. Nonrigid group theory, tunneling splittings, and nuclear spin statistics of water pentamer: $(H_2O)_5$ . *J. Phys. Chem. A* **2004**, *108*, 5527–5536. [[CrossRef](#)]
31. Longuet-Higgins, H.C. The symmetry groups of non-rigid molecules. *Mol. Phys.* **1963**, *6*, 445–460. [[CrossRef](#)]
32. Temme, F.P. Natural embedding of group in NMR spin algebras: I. Roles of model  $\lambda \vdash n$  permutational modules and their related Kostka  $A_{\lambda \mu}$  in the NMR of exo-cage clusters. *Mol. Phys.* **1995**, *85*, 883–905. [[CrossRef](#)]
33. Balasubramanian, K. Computational multinomial combinatorics for colorings of 5D-hypercubes for all irreducible representations and applications. *J. Math. Chem.* **2019**, *57*, 655–689. [[CrossRef](#)]
34. Balasubramanian, K. A method for nuclear spin statistics in molecular spectroscopy. *J. Chem. Phys.* **1981**, *74*, 6824–6829. [[CrossRef](#)]
35. Balasubramanian, K. Operator and algebraic methods for NMR spectroscopy. I. Generation of NMR spin species. *J. Chem. Phys.* **1983**, *78*, 6358–6368. [[CrossRef](#)]
36. Balasubramanian, K. Generators of the character tables of generalized wreath product groups. *Theor. Chim. Acta* **1990**, *78*, 31–43. [[CrossRef](#)]
37. Balasubramanian, K. Applications of combinatorics and graph theory to spectroscopy and quantum chemistry. *Chem. Rev.* **1985**, *85*, 599–618. [[CrossRef](#)]
38. Balasubramanian, K. Computational Enumeration of Colorings of Hyperplanes of Hypercubes for all Irreducible Representations and Applications. *J. Math. Sci. Model.* **2018**, *1*, 158–180. [[CrossRef](#)]
39. Balasubramanian, K. Computations of Colorings 7D-Hypercube's Hyperplanes for All Irreducible Representations. *J. Comput. Chem.* **2020**, *41*, 653–686. [[CrossRef](#)]
40. Balasubramanian, K. Computational combinatorics of hyperplane colorings of 6D-hypercube for all irreducible representations and applications. *J. Math. Chem.* **2020**, *58*, 204–272. [[CrossRef](#)]
41. Arockiaraj, M.; Mushtaq, S.; Klavzar, S.; Fiona, J.C.; Balasubramanian, K. Szeged-like Topological Indices and the Efficacy of the Cut Method: The Case of Melem Structures. *Discret. Math. Lett.* **2022**, *9*, 49–56. [[CrossRef](#)]
42. Arockiaraj, M.; Clement, J.; Balasubramanian, K. Topological indices and their applications to circumcised donut benzenoid systems, kekulenes and drugs. *Polycycl. Aromat. Compd.* **2020**, *40*, 280–303. [[CrossRef](#)]
43. Balasubramanian, K. Density Functional and Graph Theory Computations of Vibrational, Electronic and Topological Properties of Porous Nanographenes. *J. Phys. Organ. Chem.* **2022**, e4435. [[CrossRef](#)]
44. Klein, D.J.; Randić, M. Resistance distance. *J. Math. Chem.* **1993**, *12*, 81–95. [[CrossRef](#)]
45. Yang, Y.J.; Klein, D.J. A recursion formula for resistance distances and its applications. *Discret. Appl. Math.* **2013**, *161*, 2702–2715.
46. Graovac, A.; Pisanski, T. On the Wiener index of a graph. *J. Math. Chem.* **1991**, *8*, 53–62. [[CrossRef](#)]
47. Darafsheh, M.R. Computation of topological indices of some graphs. *Acta Appl. Math.* **2010**, *110*, 1225–1235. [[CrossRef](#)]
48. Ghorbani, M. Remarks on the Balaban Index. *Serdica J. Comput.* **2013**, *7*, 25–34. [[CrossRef](#)]
49. Liu, J.; Cao, J.; Pan, X.F.; Elaiw, A. The Kirchhoff index of hypercubes and related complex networks. *Discr. Dyn. Nat. Soc.* **2013**, *2013*, 543189. [[CrossRef](#)]
50. Daneshvar, S.; Izbirak, G.; Kaleibar, M.M. Topological indices of hypercubes. *J. Basic Appl. Res.* **2012**, *2*, 11501–11505.
51. Kaatz, F.H.; Bultheel, A. Dimensionality of hypercube clusters. *J. Math. Chem.* **2016**, *54*, 33–43. [[CrossRef](#)]
52. Diudea, M.V.; Pirvan-Moldovan, A.; Pop, R.; Medeleanu, M. Energy of graphs and remote graphs, in hypercubes, rhombellanes and fullerenes. *MATCH Commun. Math. Comput. Chem.* **2018**, *80*, 835–852.
53. Graham, N.; Harary, F. The number of perfect matchings in a hypercube. *Appl. Math. Lett.* **1988**, *1*, 45–48. [[CrossRef](#)]
54. Östergård, P.R.; Pettersson, V.H. Enumerating perfect matchings' in  $n$ -cubes. *Order* **2013**, *30*, 821–835. [[CrossRef](#)]
55. Harary, F. *Graph Theory*; Addison-Wesley: Reading, MA, USA, 1969.
56. Balasubramanian, K. The Use of Frames Method for the Characteristic-Polynomials of Chemical Graphs. *Theor. Chim. Acta* **1984**, *65*, 49–58.
57. Balasubramanian, K. Computer-Generation of the Characteristic-Polynomials of Chemical Graphs. *J. Comput. Chem.* **1984**, *5*, 387–394. [[CrossRef](#)]
58. Balasubramanian, K. TopoChemie-2020 A Fortran 95 Package 95 (Software), A Computational Package for Computing Topological Indices, Spectral Polynomials, Walks and Distance Degree Sequences and Combinatorial Generators. 2020. Available online: <https://scholar.google.com/scholar?cluster=11353625766326506250&hl=en&oi=scholar> (accessed on 16 February 2023).
59. Balasubramanian, K. Computer-Generation of Hadamard-Matrices. *J. Comput. Chem.* **1993**, *14*, 603–619. [[CrossRef](#)]

60. Ramaraj, R.; Balasubramanian, K. Computer generation of matching polynomials of chemical graphs and lattices. *J. Comput. Chem.* **1985**, *6*, 122–141. [[CrossRef](#)]
61. Bloom, G.S.; Kennedy, J.W.; Quintas, L.V. Some Problems Concerning Distance and Path Degree Sequences. In *Graph Theory*; Springer: Berlin/Heidelberg, Germany, 1983; pp. 179–190.
62. Collado, J.A. On the calculation of the spectrum of large Hückel matrices, representing carbon nanotubes, using fast Hadamard and symplectic transforms. *Mol. Phys.* **2006**, *104*, 3111–3117. [[CrossRef](#)]
63. Hosoya, H. Matching and symmetry. *Comput Math.* **1986**, *12B*, 271–290.
64. Hosoya, H.; Motoyama, A. An effective algorithm for obtaining polynomials for dimer statistics. Application of operator technique on the topological index to two-and three-dimensional rectangular and torus lattices. *J. Math. Phys.* **1985**, *26*, 157–167. [[CrossRef](#)]
65. Hosoya, H. Topological index. A newly proposed quantity characterizing the topological nature of structural isomers of saturated hydrocarbons. *Bull. Chem. Soc. Jpn.* **1971**, *44*, 2332–2339. [[CrossRef](#)]
66. Hosoya, H.; Balasubramanian, K. Computational Algorithms for Matching Polynomials of Graphs from the Characteristic Polynomials of Edge-Weighted Graphs. *J. Comput. Chem.* **1989**, *10*, 698–710. [[CrossRef](#)]
67. Hosoya, H.; Balasubramanian, K. Exact Dimer Statistics and Characteristic-Polynomials of Cacti Lattices. *Theor. Chim. Acta* **1989**, *76*, 315–329. [[CrossRef](#)]
68. Rajan, R.S.; Kumar, K.J.; Shantrinal, A.A.; Rajalaxmi, T.M.; Rajasingh, I.; Balasubramanian, K. Biochemical and phylogenetic networks-I: Hypertrees and corona products. *J. Math. Chem.* **2021**, *59*, 676–698. [[CrossRef](#)] [[PubMed](#)]
69. Balasubramanian, K. Nonrigid water octamer: Computations with the 8-cube. *J. Comput. Chem.* **2020**, *41*, 2469–2484. [[CrossRef](#)] [[PubMed](#)]
70. Sloane, N.J.A. Sequence A192437, Online Encyclopaedia of Integer Sequences. Available online: <https://oeis.org/A192437> (accessed on 28 January 2023).

**Disclaimer/Publisher’s Note:** The statements, opinions and data contained in all publications are solely those of the individual author(s) and contributor(s) and not of MDPI and/or the editor(s). MDPI and/or the editor(s) disclaim responsibility for any injury to people or property resulting from any ideas, methods, instructions or products referred to in the content.